THE JOURNAL OF BIOLOGICAL CHEMISTRY VOL. 289, NO. 21, pp. 15052–15063, May 23, 2014

Guanine Nucleotide-binding Protein (Gα) Endocytosis by a Cascade of Ubiquitin Binding Domain Proteins Is Required for Sustained Morphogenesis and Proper Mating in Yeast*[S]

Received for publication, March 16, 2014, and in revised form, April 7, 2014 Published, JBC Papers in Press, April 10, 2014, DOI 10.1074/jbc.M114.566117

Gauri Dixit[‡1], **Rachael Baker**[‡1], **Carly M. Sacks**[§], **Matthew P. Torres**[¶], **and Henrik G. Dohlman**[‡‖2]

From the [‡]*Department of Biochemistry and Biophysics,* [§]*Department of Biology, and* [‖]*Department of Pharmacology, University of North Carolina at Chapel Hill, Chapel Hill, North Carolina 27599 and* [¶]*School of Biology, Georgia Institute of Technology, Atlanta, Georgia 30332*

Background: The yeast Gα protein contains a unique domain that is monoubiquitinated, leading to vacuolar degradation.
Results: A gene deletion screen reveals ubiquitin binding domain proteins necessary for Gα trafficking. Loss of the ubiquitination domain impedes cellular morphogenesis and mating.
Conclusion: Proper endocytosis of Gα is required for sustained morphogenesis and efficient mating.
Significance: Gα endocytosis promotes signaling.

Heterotrimeric G proteins are well known to transmit signals from cell surface receptors to intracellular effector proteins. There is growing appreciation that G proteins are also present at endomembrane compartments, where they can potentially interact with a distinct set of signaling proteins. Here, we examine the cellular trafficking function of the G protein α subunit in yeast, Gpa1. Gpa1 contains a unique 109-amino acid insert within the α-helical domain that undergoes a variety of post-translational modifications. Among these is monoubiquitination, catalyzed by the NEDD4 family ubiquitin ligase Rsp5. Using a newly optimized method for G protein purification together with biophysical measures of structure and function, we show that the ubiquitination domain does not influence enzyme activity. By screening a panel of 39 gene deletion mutants, each lacking a different ubiquitin binding domain protein, we identify seven that are necessary to deliver Gpa1 to the vacuole compartment including four proteins (Ede1, Bul1, Ddi1, and Rup1) previously not known to be involved in this process. Finally, we show that proper endocytosis of the G protein is needed for sustained cellular morphogenesis and mating in response to pheromone stimulation. We conclude that a cascade of ubiquitin-binding proteins serves to deliver the G protein to its final destination within the cell. In this instance and in contrast to the previously characterized visual system, endocytosis from the plasma membrane is needed for proper signal transduction rather than for signal desensitization.

Gα proteins are enzymatic switches that are part of a multicomponent signaling complex. The complex typically consists of a seven-transmembrane G protein-coupled receptor, a guanine nucleotide-binding protein (Gα), and an associated dimer consisting of β and γ subunits (Gβγ) (1). Signaling is turned on and off based on receptor activation, which in turn dictates the nucleotide-bound state of the Gα protein. When Gα is GDP-bound, Gβγ is sequestered, and signaling pathways are off (1). When Gα releases GDP and binds GTP, Gβγ dissociates, and the signaling pathways are turned on. Subsequent GTP hydrolysis is accelerated by regulators of G protein signaling (RGS[3] proteins) (2, 3). Large Gα proteins contain a Ras-like domain as well as an independently folded α-helical domain (1). Within this group of proteins there is a well established role for the Ras-like domain in specifying interactions with Gβγ, effectors, and RGS proteins (1). However, recent evidence has shown that the α-helical domain is also important for signal modulation (4). Accordingly, structure determinations have revealed differences in the α-helical domain of $G\alpha_i$ when bound to GDP and GTPγS (5–7).

Apart from the regulation of GTP binding and hydrolysis, G proteins are regulated by targeted delivery to subcellular compartments (8). G protein trafficking can be either constitutive or stimulus-dependent. Stimulus-dependent movement of Gα and Gβγ to various endomembrane compartments has been observed in several systems including the visual system in *Drosophila* and mammals (8, 9) as well as certain non-visual systems (10, 11). In the yeast *Saccharomyces cerevisiae*, the Gα Gpa1 is constitutively trafficked to endosomes, where it binds to and activates a phosphatidylinositol 3-kinase, as well as to the vacuole, where the protein is eventually degraded (12, 13). More recently, work by Irannejad *et al.* (14) demonstrated that mammalian $G\alpha_s$ is present and active at the endosomal membrane as well as at the plasma membrane (15). However, the functional importance of Gα trafficking is not well established (8).

* This work was supported, in whole or in part, by National Institutes of Health Grant GM101560 (to H. G. D.).
[S] This article contains supplemental Fig. S1.
[1] Both authors contributed equally to this work.
[2] To whom correspondence should be addressed: Dept. of Biochemistry and Biophysics, The University of North Carolina at Chapel Hill, Genetic Medicine Bldg., Suite 3010, Chapel Hill, NC 27599. Tel.: 919-843-6894; E-mail: hdohlman@med.unc.edu.

[3] The abbreviations used are: RGS, regulator of G protein signaling; UBD, ubiquitin binding domain; UD, ubiquitination domain; TEV, tobacco etch virus; ABD-F, 4-fluoro-7-aminosulfonylbenzoflurazan; MANT, *N*-methylanthraniloyl; UBD, ubiquitin binding domain; GTPγS, guanosine 5′-3-*O*-(thio)triphosphate.

To fully understand the consequences of G protein trafficking, we must first understand how such trafficking events are regulated. Much of the spatial control of G protein-coupled receptors and G proteins is dependent upon post-translational modification by monoubiquitination. For example, the yeast Gβ (Ste4) and G protein-coupled receptor (Ste2) are monoubiquitinated after stimulation with the mating pheromone α-factor (16–18). Both proteins are subsequently removed from the plasma membrane and delivered to the vacuole (17–19). For Ste2 this process is mediated in part by endocytic adaptor proteins containing a ubiquitin binding domain (UBD) (21, 22). Although structurally diverse, UBDs share the ability to bind non-covalently to ubiquitin-conjugated substrates and serve to transport monoubiquitinated proteins through the various stages of endocytosis (23). Although the general process of monoubiquitination-mediated endocytosis is well understood, questions remain concerning the specific protein components that are important for trafficking of the G protein.

The yeast model system, in which many ubiquitination and cellular trafficking components were originally identified, can facilitate understanding of the interconnections between G protein signaling, monoubiquitination, and trafficking (24). Pheromone binds to Ste2, which is coupled to Gpa1 (Gα) and Ste4/Ste18 (Gβγ). When Gα is activated, Gβγ dissociates and stimulates a kinase cascade leading to activation of the yeast MAPK Fus3. A second branch of the pathway leads to activation of a Rho family GTPase, Cdc42 (24). Together these processes result in cell cycle arrest, new gene transcription, and morphological changes that facilitate mating (24). Pheromone pathway signaling is attenuated by the pheromone-dependent monoubiquitination and endocytosis of the G protein-coupled receptor Ste2 (16). As with the receptor, monoubiquitination leads to the endocytosis and eventual vacuolar degradation of Gpa1 (25). In contrast to Ste2, monoubiquitination of Gpa1 is not dependent on pheromone stimulation. Both proteins are monoubiquitinated by the same ubiquitin ligase, Rsp5 (26, 27).

Although the Ras-like and α-helical domains are highly conserved across species, Gpa1 possesses a unique 109-amino acid insert (ubiquitination domain (UD)) within the α-helical domain. The UD contains the known sites of phosphorylation as well as the primary residue for both monoubiquitination and polyubiquitination (25, 26, 28–31). Given that the α-helical domain modulates the activity of some G proteins, we considered whether the UD could influence the activity as well as the cellular distribution of Gpa1. Here we show that the UD does not influence G protein catalytic activity or downstream MAPK signaling but is needed for proper trafficking of Gpa1 to the vacuole. Our screen of 39 gene deletion mutations revealed seven UBD-containing proteins that are required for Gpa1 trafficking. Four of these proteins are required for trafficking of Gpa1 but not Ste2, thus demonstrating that constitutive endocytosis of these proteins occurs by distinct mechanisms. Finally, we show that Gα endocytosis from the plasma membrane is required for sustained cellular morphogenesis and efficient mating.

EXPERIMENTAL PROCEDURES

Strains, Plasmids, and Growth of Cultures—Standard procedures were followed for the growth, maintenance, and transformation of yeast and bacteria. Proteins for biochemical studies were expressed in *Escherichia coli* BL21 (DE3) RIPL cells (Stratagene, La Jolla, CA) grown at 18 °C overnight after induction with isopropyl β-D-1-thiogalactopyranoside. The yeast (*S. cerevisiae*) strain used in this study was BY4741 (*MAT***a** *leu2*Δ *met15*Δ *his3-1 ura3*Δ) and its derivatives. Cells were grown at 30 °C in yeast extract peptone medium or synthetic complete medium containing 2% (w/v) dextrose. The *gpa1*$^{\Delta UD}$ mutant strain was generated by transformation of AflII-digested pRS406-GPA1_trunc$^{\Delta UD}$ in wild type cells. In each case transformed cells were grown in synthetic complete medium that lacked the appropriate nutrient or yeast extract peptone medium with the appropriate drug.

Plasmid Construction—Both the native (*sc*Gpa1) and codon-optimized Gpa1 (*co*Gpa1) were cloned into the bacterial expression vector pQlinkH (Addgene), which contains an N-terminal tobacco etch virus (TEV) protease-cleavable His_6 tag, using the BamHI and NotI restriction sites. Efficient TEV protease cleavage required the use of Gpa1$^{\Delta N}$ lacking the first 38 amino acids, which are predicted to be unstructured based on alignment with $G\alpha_i$ (32). pQlinkH-GPA1$^{\Delta N\Delta UD}$ was constructed by deleting the coding sequence corresponding to amino acids 128–236 from the pQlinkH-GPA1$^{\Delta N}$ plasmid. The pRS406-STE2-GFP integrating vector was constructed by PCR amplification of ~900 base pairs from the 3′ end of *STE2* in-frame with GFP from the yeast GFP strain collection (Invitrogen). Genomic DNA from the above strain was amplified with flanking KpnI and SacI sites for introduction to pRS406. The pRS406-GPA1_trunc$^{\Delta UD}$ integrating vector was constructed by PCR amplification of GPA1$^{\Delta UD}$ from pRS406-GPA1$^{\Delta UD}$-GFP minus the first 81 base pairs of GPA1. The PCR product was flanked by XbaI and SacI sites for introduction to pRS406. Site-directed mutagenesis was used to introduce a silent mutation at bp 181 to generate an AflII site for integration. Construction of the pRS406-GPA1-GFP, pRS406-GPA1$^{\Delta UD}$-GFP, pRS423-FUS1-lacZ, and pADM4-GPA1 vectors has been described previously (25, 33, 34).

Bacterial Protein Expression and Purification—Generating the quantities of pure Gpa1 necessary to complete biophysical studies has been a barrier to progress both because of low initial protein expression and impurities, necessitating additional purification steps. We optimized the process using small-scale batch purification and TEV protease-cleavage to release protein from the nickel beads (Table 1). *E. coli* were lysed by homogenization (NanoDeBee) at 1000 p.s.i. in 25 mM potassium phosphate buffer, pH 7.0, with 300 mM KCl and 250 μM tris(2-carboxyethyl)phosphine. After clarification by centrifugation, the lysate from 500 ml of cell culture was bound to 1 ml of nickel-nitrilotriacetic acid-agarose bead slurry (Qiagen) pre-equilibrated in phosphate buffer, pH 7.0, for 20 min at 4 °C. The beads were washed 3 times at 4 °C with 25 mM phosphate buffer, pH 7.0, with 300 mM KCl, then 3 times with Gpa1 buffer (25 mM phosphate buffer, pH 7.0, and 100 mM KCl) with 100 μM GDP and 500 μM tris(2-carboxyethyl)phosphine. Gpa1 was

TABLE 1

Optimization of Gpa1 purification

Construct describes the expression vector used. Induction is an estimate of the expression level of Gpa1 produced in *E. coli.* Purification, method used for His purification. Purity, percent homogeneity after His column purification. Values are estimated from SDS-PAGE and Coomassie staining. Final yield given in the last column in mg/liters. ND, not determined.

Construct	Induction	Purification	Purity	mg/l
*sc*Gpa1	+	Column	<25%	1.6
*sc*Gpa1	+	Batch	~50%	10.4
*sc*Gpa1	+	Batch with TEV	ND	ND
*sc*Gpa1$^{\Delta N}$	++	Batch with TEV	>90%	4.6
*co*Gpa1$^{\Delta N}$	++++	Batch with TEV	>90%	18

cleaved from the beads by incubation at 4 °C overnight with 500 μg of TEV protease. The final product was judged >95% pure by SDS-PAGE. Protein was stored at 4 °C (never frozen) and used within 2 days. Although the use of TEV protease cleavage to release Gpa1 decreased the yield from the first purification step (about half of the Gpa1 remains on the beads), this loss in efficiency is mitigated by the increase in purity (does not require further dialysis or purification steps). Furthermore, we found that 46% of the codons in Gpa1 are rarely used in *E. coli*, which can significantly reduce the efficiency of expression (35). A codon-optimized Gpa1 yielded 18 mg/liter, an increase of 11-fold over the original method.

Circular Dichroism—Gpa1 was diluted to 5 μM in Gpa1 buffer with 50 μM GDP, 50 μM $MgCl_2$, and 550 μM tris(2-carboxyethyl)phosphine. Spectra were recorded from 190 to 260 nm on a Chirascan plus CD spectrometer at 25 °C using a 1-mm quartz cell. Buffer background was subtracted from the spectra.

Quantitative Mass Spectrometry of ABD-labeled Cysteines—Gpa1$^{\Delta N}$ was diluted to 2 μM in Gpa1 buffer with 50 μM GDP or GTPγS. Protein sample was mixed with 4-fluoro-7-aminosulfonylbenzoflurazan (ABD-F, Anaspec) on ice (final concentration, 2 mM). 20-μl aliquots of the sample were reacted for 3 min at either 42 °C or 70 °C and then transferred to ice to quench ABD-F labeling. Samples were prepared for mass spectrometry and analyzed as described by Isom *et al.* (36). Data collected on a Nano-Acquity HPLC solvent delivery system (Waters Corp.) connected through an electrospray ionization source interfaced to an LTQ Orbitrap Velos ion trap mass spectrometer (Thermo Electron Corp.).

Thermal Stability of Gpa1—The fast quantitative cysteine reactivity method (37) was employed to measure Gpa1 thermal stability. Briefly, 2 μM protein was incubated with 1 mM ABD-F in Gpa1 buffer in the presence of 20 μM GDP or GTPγS and 2 mM $MgCl_2$ at the desired temperature for 3 min. The reaction was quenched with 20 mM HCl (final concentration), and ABD-F fluorescence was measured on a PHERAstar plate reader (BMG Labtech, excitation at 400 nm and emission at 500 nm). The data were normalized and fit using GraphPad Prism (GraphPad Software; San Diego, CA) to determine the temperature at which half the protein was unfolded, representing the melting temperature (T_m).

Nucleotide Dissociation Assay—Purified Gpa1 was exchanged into Gpa1 buffer with 50 μM $MgCl_2$ and 100 μM GDP. To initiate association, 1 μM 2′-*O*-(*N*-methylanthraniloyl)-guanosine 5′-diphosphate (MANT-GDP) was added to 1 μM protein at room temperature. Gpa1 was determined to be fully loaded when the fluorescence intensity reached a maximum (~250 s). Association was measured as a change in fluorescence intensity over time (excitation, 360 nm; emission, 440 nm) using a LS50B PerkinElmer Life Sciences Luminescence Spectrometer. MANT-GDP dissociation was initiated by the addition of 500 μM unlabeled GDP. Fluorescence data were fit in GraphPad Prism to a one-phase exponential association or decay curve.

Intrinsic GTP Binding and Hydrolysis—Purified Gpa1 (200 nM) was equilibrated to room temperature in Gpa1 buffer with 50 μM $MgCl_2$. GTP at a final concentration of 200 nM was added, and GTP binding and hydrolysis were monitored by the change in intrinsic fluorescence of Gpa1 that occurs upon rearrangement of the tryptophan near the nucleotide binding region (excitation at 284 nm and emission at 340 nm) using a LS50B PerkinElmer Life Sciences Luminescence Spectrometer. Data were fit to exponential association or dissociation curves using GraphPad Prism.

Microscopy Screen for Gpa1 and Ste2 Trafficking—BY4741-derived mutants lacking specific ubiquitin binding domain-containing proteins (disrupted using the KanMX G418 resistance marker, from Research Genetics, Huntsville, AL) were used for the screen. *PEP4* was disrupted in the deletion mutant strains by single-step gene replacement with *pep4*::*HIS3* using PCR-mediated gene disruption (38). *GPA1*-GFP was introduced in each strain by transformation of pRS406-GPA1-GFP after digestion with HindIII (25). Separately, *STE2*-GFP was introduced in the deletion mutants by transformation of pRS406-STE2-GFP (this study) after digestion with AfeI. Screen hits (deletion mutants that mislocalized Gpa1-GFP) were re-made in BY4741 and BY4741-derived strains by gene replacement with KanMX4 using PCR and pFA6KanMX as the template (39). All deletions were verified by PCR and nucleotide sequence analysis and analyzed for Gpa1-GFP localization.

Transcriptional Reporter Assays—Pheromone sensitivity was measured by a transcriptional reporter assay (33) as described earlier. Briefly, cells transformed with pRS423 FUS1-LacZ were stimulated with different concentrations of pheromone for 90 min. β-Galactosidase activity was measured spectrophotometrically (750 nm) using fluorescein di-β-D-galactopyranoside as the substrate.

Protein Detection—Yeast cells either untreated or treated with 3 μM α-factor for 30 min were harvested in trichloroacetic acid (TCA, 5% final concentration), centrifuged, washed with 10 mM NaN_3, and pellets were frozen at −80 °C. Cell extracts were prepared by glass bead lysis in TCA as previously described (40). Protein concentrations were determined by a Bradford colorimetric protein assay (Bio-Rad). 25 μg of protein (40 μg to evaluate Gpa1 ubiquitination) was resolved by 10% SDS-PAGE, transferred to nitrocellulose, and detected by immunoblotting with antibodies for phospho-p44/42 MAPK at 1:500 (9101L; Cell Signaling Technology), Fus3 at 1:500 (sc-6773; Santa Cruz Biotechnology), G6PDH at 1:50,000 (A9521, Sigma), and Gpa1 at 1:1,000 (41). Immunoreactive species were visualized by chemiluminescence detection (PerkinElmer Life Sciences) of horseradish peroxidase-conjugated anti-rabbit (sc 170-5046) or anti-goat (sc-2768) at 1:10,000. Blots were either scanned using Typhoon Trio+ (GE Healthcare) or developed

by film exposure on HyBlot Cl autoradiography film (Denville Scientific), and band intensity was quantified using Fiji (National Institutes of Health).

Time-lapse Imaging in Microfluidics Chambers—A microfluidics device similar to the one described earlier was constructed (42). Early-mid log phase yeast cells were loaded in the chamber and stimulated with the indicated concentration of α-factor pheromone. Differential interference contrast images were acquired every 5 min for 8 h using a 60× PlanApo objective under oil immersion. Images were captured using an Olympus Spinning disc confocal microscope equipped with a motorized XYZ stage and photometrics EM CCD camera. Image processing and analysis was done using ImageJ software.

Quantitative Mating Efficiency Assay—The mating assay was performed as previously described (43). Equal amounts of early-log phase *MAT***a** cells (BY4741) and *MATα* cells (BY4742, *leu2*Δ *his3*Δ *ura3*Δ *lys2*Δ) were mixed, sterile-filtered onto nitrocellulose membranes, and overlaid onto yeast extract peptone medium plates at 30 °C for 4 h. Cells were diluted and plated onto synthetic complete medium and synthetic dextrose medium with only His, Ura, and Leu to select for diploids. Mating efficiency was calculated by dividing the number of diploid colonies by the total number of colonies on the synthetic complete medium plate.

RESULTS

Structural Contributions of the Ubiquitination Domain to Gpa1—Gpa1 is distinct from other Gα proteins because of the UD. A comparison of available genome sequences shows that the UD is found among Saccharomycotina but is not present in other eukaryotes (Fig. 1*A* and supplemental Fig. 1). Based on sequence alignment with Gα proteins, the UD is at the end of the A/B helix in the α-helical domain (Fig. 1*B*). Previous analysis has shown that the UD is the site of post-translational modifications including phosphorylation, monoubiquitination, and polyubiquitination (25, 26, 28–31).

To be modified, amino acids must be accessible to the modifying enzyme. The ability to modify a given amino acid requires that the residue be present at the surface of the protein or in a region lacking secondary structure. Indeed, phosphorylation and ubiquitination often occur on intrinsically disordered regions of proteins (44). Therefore, we postulated that the UD is without substantial secondary structure. To test our hypothesis we employed a series of biophysical measurements of protein conformation. First, we used circular dichroism to determine the contribution of the UD to the secondary structure content of Gpa1. This analysis revealed no difference between Gpa1 with or without the UD (Fig. 1*C*). Precise removal of the UD resulted in expression comparable with that of the full-length protein, whereas removing just one additional amino acid abolished expression entirely. We infer that the UD does not contribute to the structure of the adjoining helical domain.

To further assess whether the UD contains unfolded regions, we asked whether resident cysteines were especially accessible to labeling with a small modifier ABD-F (36). Gpa1 is an ideal candidate for this method because it contains cysteines dispersed throughout the protein. There are two in the Ras-like domain (Cys-333 and Cys-443), four in the helical domain (Cys-105, Cys-117, Cys-258, and Cys-288), and one in the UD (Cys-208). Using this method, we detected ABD-F labeling for five of the seven cysteines. As seen in Fig. 1*D*, cysteines within the well folded helical domain are highly protected, whereas the cysteine in the UD is highly exposed (value close to one). These results are consistent with the circular dichroism data, suggesting that the UD lacks secondary structure. Taken together, our results are consistent with the hypothesis that the UD is an evolutionarily unique, structurally distinct, and largely unstructured domain.

Functional Contributions of the Ubiquitination Domain to Gpa1 Activity—The α-helical domain is known to influence G protein nucleotide exchange activity (45). The UD is adjacent to the A/B helix of the helical domain, a region whose dynamics were previously shown to promote the rapid, receptor-independent, nucleotide exchange activity of *Arabidopsis thaliana* Gα (45). However, it is not known whether the UD regulates the enzymatic activity of *S. cerevisiae* Gpa1. To address this question we used the cysteine reactivity method to measure the thermal stability of Gpa1 in the presence and absence of the UD. As shown in Fig. 2*A*, removing the UD did not alter Gpa1 thermal stability despite the loss of 109 amino acids. We then measured the ability of guanine nucleotides to bind Gpa1 in the presence and absence of the UD. For these experiments we used the fluorescent nucleotide analog MANT-GDP. The rate of nucleotide exchange was measured as a loss of fluorescence over time as Gpa1 released MANT-GDP and bound unlabeled GDP, added in excess. As shown in Fig. 2*B*, the rate of nucleotide dissociation was not altered by the absence of the UD. Finally, we measured the rate of GTP hydrolysis using a method that monitors a nucleotide-dependent change in the intrinsic fluorescence of Gpa1 (46). Using this assay, we observed similar rates of GTP hydrolysis in the presence and absence of the UD (Fig. 2*C*). Together, these data suggest that the UD does not alter the structure or enzymatic activity of Gpa1.

A Cascade of Ubiquitin Binding Domain Proteins Transport Gpa1 to the Vacuole—The data presented above indicate that the UD does not directly contribute to the structure and enzymatic function of Gpa1. However, the UD functions as a site of phosphorylation, polyubiquitination (for targeting to the proteasome), and monoubiquitination (for trafficking to the vacuole) (25, 26, 28–31). Gpa1 is monoubiquitinated by the Rsp5 ubiquitin ligase (26). However, the proteins involved in Gpa1 endocytosis and specifically those that recognize monoubiquitin within the UD are not known. Accordingly, we embarked on a search for proteins that recognize the monoubiquitinated form of Gpa1.

Monoubiquitin-mediated trafficking pathways are often composed of ubiquitin binding domain (UBD)-containing proteins (47). In most cases, multiple UBD-containing proteins are involved in the passage of a monoubiquitinated protein to its final destination (23). Moreover, the route of endocytosis appears to be dictated in part by the identity of the monoubiquitinated protein (23). Numerous UBDs have been previously defined (48) and are now included in the protein descriptions found in the Saccharomyces Genome Database (SGD; www.yeastgenome.org). Using UBD proteins known at the start of this project, we screened a comprehensive set of gene deletion

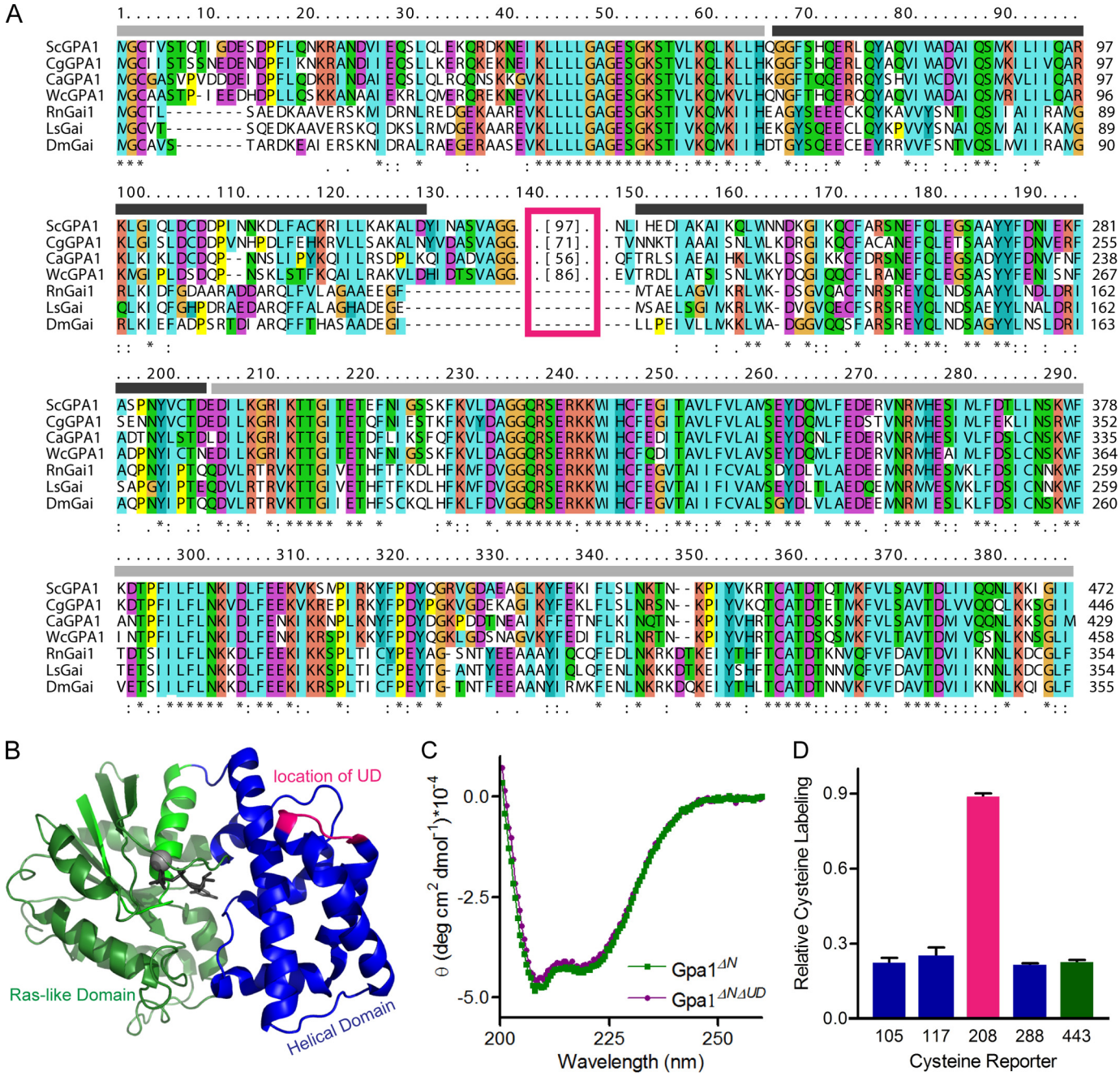

FIGURE 1. **Conservation of the ubiquitination domain.** *A*, sequence alignment of Gpa1-like Gα proteins from yeast *S. cerevisiae* (*Sc*), other Saccharomycotina (*Candida glabrata* (*Cg*), *Candida albicans* (*Ca*), *Wickerhamomyces ciferrii* (*Wc*)) as well as $G\alpha_i$ from rat (*Rattus norvegicus* (*Rn*)), snail (*Lymnaea stagnalis* (*Ls*)) and fruit fly (*Drosophila melanogaster* (*Dm*)). The *gray bar* indicates the Ras-like domain; the *black bar* indicates the helical domain. Location of the insert within the helical domain is highlighted with a *magenta box*. The number of amino acids in the *inset* is given in *parentheses*. *B*, structure of $G\alpha_i$ (PDB code 1GIA) showing the location of the Gpa1 ubiquitination domain (*magenta*) based on the sequence alignment. The Ras-like domain is shown in *green*, and the α-helical domain is shown in *blue*. Magnesium and the GTP analog shown are in *gray*. *C*, secondary structure content of $Gpa1^{\Delta N}$ and $Gpa1^{\Delta N\Delta UD}$ measured by circular dichroism. *D*, relative labeling of five cysteines in GTPγS-bound Gpa1. Results are the mean ± S.E. Coloring is according to that used in *B*.

strains for endocytosis and trafficking defects affecting the delivery of Gpa1 from the plasma membrane to the vacuole. Because Gpa1 and Ste2 are targeted for internalization by the same ubiquitin ligase, we also examined trafficking of Ste2, with the expectation that both proteins share the same trafficking machinery components. Accordingly, we monitored the localization of GFP-tagged Gpa1 (Gpa1-GFP) and Ste2 (Ste2-GFP) in a total of 39 UBD deletion strains (49, 50). Gpa1-GFP was introduced in a strain lacking the master vacuolar protease (*pep4*Δ) so as to preserve the GFP signal after delivery to the vacuole (25). Ste2-GFP was expressed from the native *STE2* locus.

As a proof of concept we first monitored GFP localization in the absence of Vps23, Vps27, Vps9, or Rpn10. Major trafficking defects were observed for both Gpa1-GFP and Ste2-GFP in the absence of Vps23 or Vps27, two known components of the ESCRT (Endosomal Sorting Complexes Required for Transport) machinery (Fig. 3) (51, 52). Trafficking defects were also

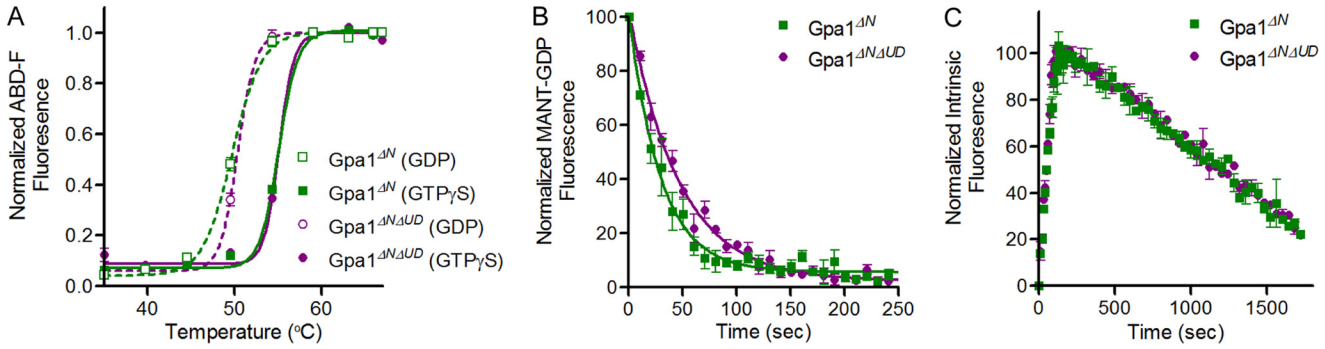

FIGURE 2. **The ubiquitination domain does not contribute to Gpa1 activity.** *A*, thermal stability of Gpa1$^{\Delta N}$ and Gpa1$^{\Delta N\Delta UD}$ measured by ABD-F labeling and fast quantitative cysteine reactivity. Data were normalized to the maximum fluorescence intensity for each curve, and results are the mean ± S.E. ($n = 4$). *B*, intrinsic nucleotide dissociation rates for Gpa1$^{\Delta N}$ and Gpa1$^{\Delta N\Delta UD}$ pre-loaded with MANT-GDP. The rate of GDP dissociation was monitored as a decrease in MANT-GDP fluorescence upon the addition of unlabeled GDP. Data are fit to an exponential dissociation curve. Results are the mean ± S.E. ($n = 3$). *C*, intrinsic tryptophan fluorescence measure of GTP binding and hydrolysis for Gpa1$^{\Delta N}$ and Gpa1$^{\Delta N\Delta UD}$. Data are normalized to the maximum signal achieved in each experiment upon completion of binding. Results are the mean ± S.E. ($n = 3$).

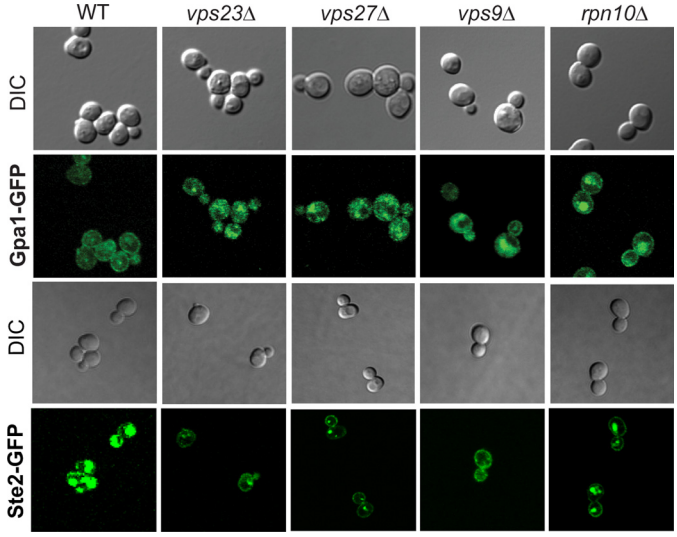

FIGURE 3. **Vacuolar protein sorting complex proteins that disrupt trafficking of Gpa1 and Ste2.** Differential interference contrast (*DIC*) and GFP images showing Gpa1-GFP and Ste2-GFP in the absence of ESCRT complex proteins Vps23 and Vps27; only Ste2-GFP trafficking is disrupted in the absence of Vps9. Trafficking of neither Gpa1 nor Ste2 is affected in the absence of the polyubiquitin binding proteasomal protein (*rpn10*Δ).

observed for Ste2-GFP after deletion of Vps9, a protein required for efficient endocytic trafficking of proteins (53). Finally, deletion of the polyubiquitin binding proteasomal protein Rpn10 did not affect trafficking of the receptor or G protein (Fig. 3), indicating that the screen specifically monitors the fate of monoubiquitinated proteins.

Having validated the screening approach, we conducted a more comprehensive screen of the known UBD-containing proteins in yeast (Fig. 4*A*). Our general strategy was to look for UBD mutants that prevent accumulation of GFP in the vacuole. As shown in Fig. 4*B*, vacuoles were visualized by pulse-staining with an amphiphilic styryl dye (FM4-64, *red*), which initially incorporates into the plasma membrane and gradually accumulates in the lumen of the vacuole (54). In wild type cells Gpa1-GFP was present at the plasma membrane but not in vacuoles, consistent with our previous findings (25) (Fig. 4*B*, *left*). In *pep4*Δ cells Gpa1-GFP accumulated in the vacuole, indicative of monoubiquitin-dependent vacuolar translocation (Fig. 4*B*, *middle*). Of the 39 UBD deletion strains tested, seven exhibited Gpa1-GFP mislocalized to puncta within the cytoplasm (Fig. 4*B*, *right*). Major trafficking defects were observed in the absence of Vps36, a component of the ESCRT machinery (51). Additionally, defects in Gpa1 localization were seen upon deletion of the following: Bul1, the ubiquitin binding component of the Rsp5 ubiquitin ligase (55); Ede1, a component of the early endocytic machinery (56); Ddi1, a DNA damage inducible v-SNARE-binding protein regulating exocytosis (57); Rup1, a regulator of Rsp5 (58) (Fig. 4*C*). Defects in Ste2-GFP trafficking were likewise observed in the absence of Vps36. However, four of the UBD deletions that affected Gpa1 trafficking had no effect on Ste2 endocytosis (Fig. 4*D*). In total, we identified seven UBD proteins necessary for proper vacuolar delivery of Gpa1 (Figs. 3 and 4). Deletion of four of these proteins disrupted trafficking of Gpa1 but not Ste2, indicating that their trafficking pathways differ. Alternatively, there could be a high degree of functional redundancy among UBDs in regulating Ste2, but not Gpa1, trafficking.

Gpa1 Is Delivered to the Plasma Membrane in the Absence of UBD Proteins Involved in Endocytosis—Having identified mutants that alter the cellular distribution of Gpa1, we next considered whether the defect was due to removal from, or delivery to, the plasma membrane. That is, Gpa1 mislocalization could be caused by impaired synthesis, maturation, or delivery to the plasma membrane. To rule out this possibility we compared the localization of Gpa1 with that of Gpa1$^{\Delta UD}$, which in wild type cells is delivered to the plasma membrane but not the vacuole (25). For all the UBD mutants tested, we found that Gpa1$^{\Delta UD}$-GFP was localized normally to the plasma membrane (Fig. 5). These data indicate that the UBD-containing proteins identified in our screen are specifically required for trafficking of monoubiquitinated Gpa1 from the plasma membrane to the vacuole.

Disruption of Gpa1 Trafficking Promotes Accumulation of Ubiquitinated Gpa1—Post-translational modification by monoubiquitination and polyubiquitination are used to regulate the quantity of Gpa1 present at the plasma membrane. Whereas monoubiquitinated Gpa1 is delivered to the vacuole, where it is eventually degraded, polyubiquitinated Gpa1 is recruited to the proteasome, where it is likewise degraded. We reasoned that disruption of Gpa1 trafficking might allow the

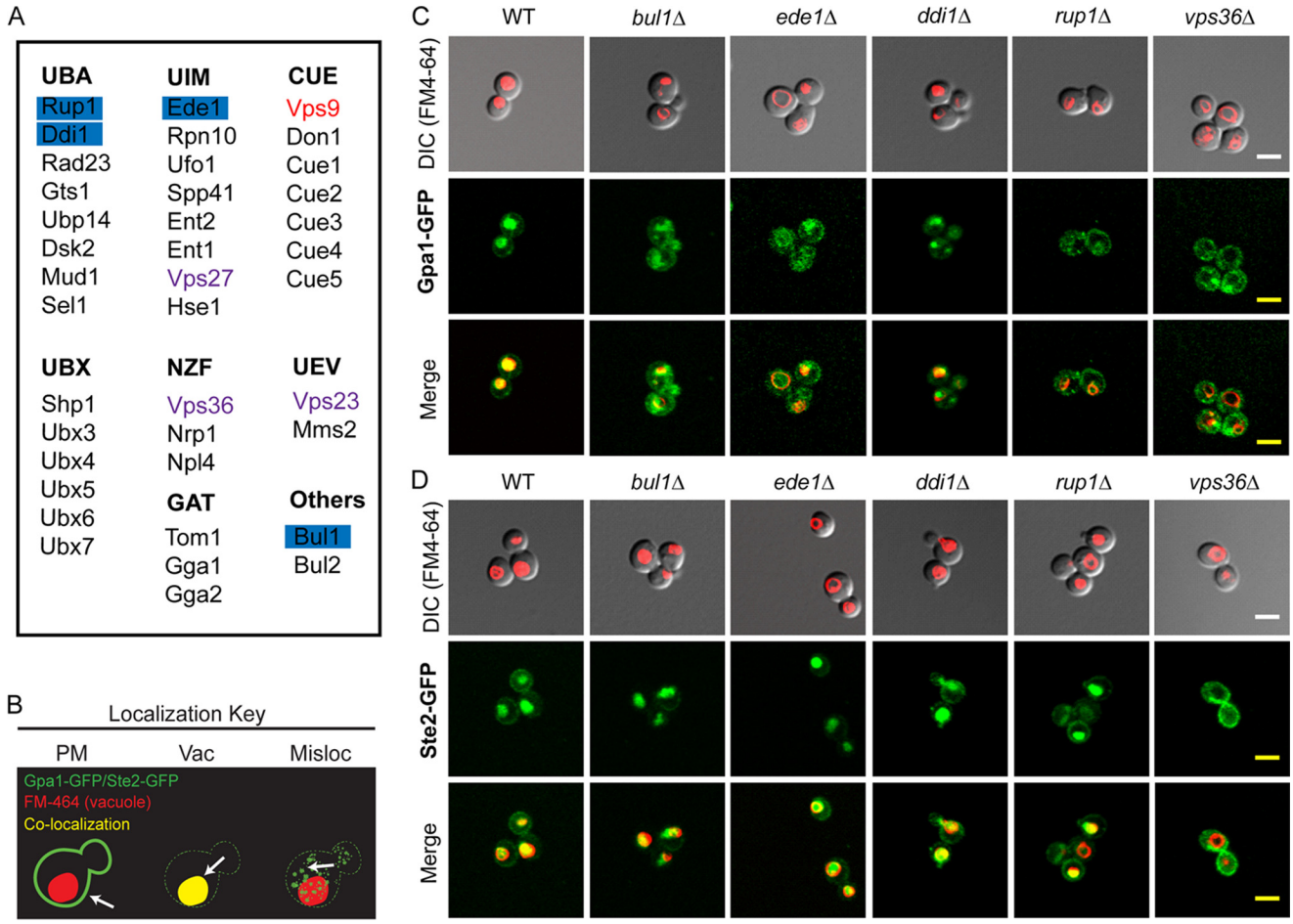

FIGURE 4. **Screen for Gpa1 translocation mutants identifies components of the endocytosis and vacuolar trafficking machinery.** *A*, table of all UBD-containing proteins screened. Proteins are sorted by the type of UBD they contain: *UBA*, ubiquitin associated; *UIM*, ubiquitin interacting motif; *CUE*, coupling of ubiquitin conjugation to endoplasmic reticulum; *UBX*, ubiquitin regulatory X; *NZF*, Npl4 zinc finger; *GAT*, [GGA(Golgi-localized, gamma-ear containing) ADP-ribosylation factor-binding protein, and TOM (target of Myb)]; *UEV*, ubiquitin-conjugating enzyme E2 variant. *B*, general scheme of the genetic screen to identify binding partners of Gpa1-ubiquitin. A total of 39 deletion mutants, each lacking a specific UBD-containing protein, were separately transformed with plasmids encoding either Gpa1-GFP (pRS406-GPA1-GFP) or Ste2-GFP (pRS406-STE2-GFP). Gpa1 and Ste2 localization was monitored by differential interference contrast and fluorescence microscopy in the presence of a vacuolar dye (*red*, FM4-64). In the absence of endocytosis the proteins were retained at the plasma membrane (*PM*; *green*, *left*). After delivery to the vacuole (*Vac*), the proteins colocalized with FM4-64 (*yellow*, *middle*). If trafficking was disrupted at any point, the proteins were mislocalized (*Misloc*) to puncta in the cytoplasm (*right*). Microscopy of mutants that mislocalized Gpa1-GFP (*C*) but not Ste2-GFP (*D*) is shown. Mutant *vps36*Δ is shown as an example of a UBD that affects trafficking of both Gpa1 and Ste2. Scale bar, 5 μm.

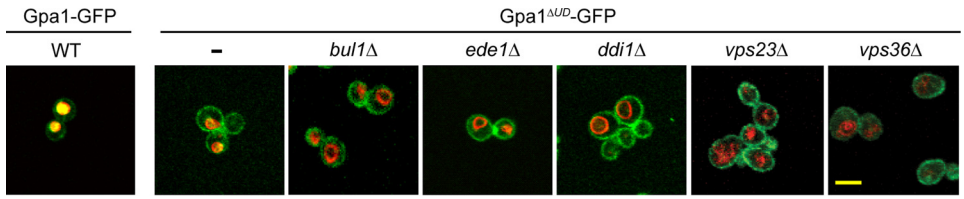

FIGURE 5. **Components of the Gpa1 trafficking machinery do not affect delivery of Gpa1 to the plasma membrane.** Microscopy of full-length Gpa1-GFP or Gpa1 lacking the ubiquitination domain (Gpa1$^{\Delta UD}$-GFP) in the presence (WT) or absence (*bul1*Δ, *ede1*Δ, *ddi1*Δ, *vps36*Δ, *vps23*Δ) of the indicated UBD proteins. Vacuoles are stained with FM4-64. *Scale bar*, 5 μm. Despite repeated attempts, we were unable to delete *RUP1* in the Gpa1$^{\Delta UD}$ background.

monoubiquitinated protein to accumulate and perhaps undergo additional rounds of ubiquitination. To test our hypothesis we monitored the level of Gpa1 ubiquitination in the four UBD deletion mutants that exhibited trafficking defects for Gpa1 (but not Ste2). To visualize the rare monoubiquitinated species we overexpressed Gpa1 using a multicopy plasmid (28). As expected we observed an increase of monoubiquitinated Gpa1 in three of the four UBD deletions (*ede1*Δ, *ddi1*Δ, and *rup1*Δ). The increase was similar to that seen upon deletion of *PEP4*, consistent with a defect in vacuolar degradation of Gpa1 (Fig. 6). Additionally, we observed an increase in polyubiquitinated Gpa1, particularly upon deletion of *EDE1* (Fig. 6). The increase in monoubiquitinated Gpa1 was not due to an overall increase in the amount of loaded substrate protein, as evident from shorter exposures of the blot. These data suggest that disruption of Gpa1 trafficking slows the clearance of monoubiquitinated Gpa1 and drives the system toward polyubiquitination (26).

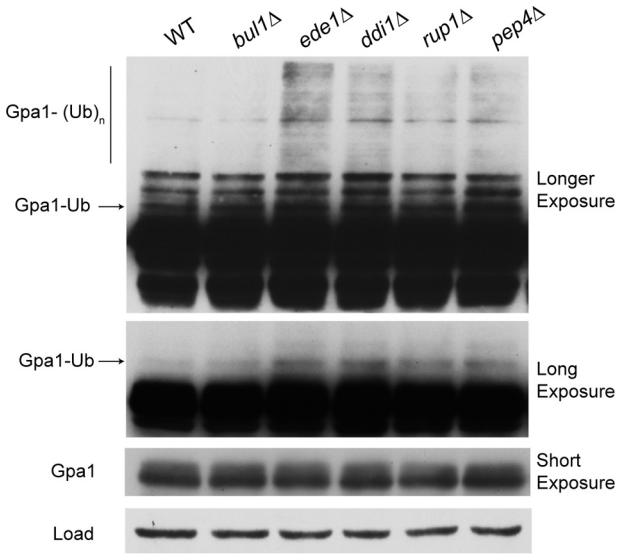

FIGURE 6. **Disruption of Gpa1 trafficking leads to accumulation of ubiquitinated Gpa1.** Gpa1 was overexpressed (pAD4M-GPA1) in the presence (*WT*) or absence (*bul1*Δ, *ede1*Δ, *ddi1*Δ, *rup1*Δ, and *pep4*Δ) of the indicated proteins and analyzed by immunoblotting with Gpa1 antibodies. *Uppermost panels* are identical except for exposure time. *Bottom*, immunoblotting with G6PDH antibodies (*Load*) as a control.

Retention of Gpa1$^{\Delta UD}$ at the Plasma Membrane Inhibits Proper Morphogenesis and Mating—Previous studies revealed that persistent GTP activation leads to an accumulation of Gpa1 at endosomes (12). Conversely, removal of the UD leads to an accumulation of Gpa1 at the plasma membrane (25). With the availability of the Gpa1$^{\Delta UD}$ mutant, as well as UBD mutants that disrupt translocation of the wild type protein, we have the ability to study the functional consequences of Gpa1 trafficking without the confounding effects of altered GTPase activity. Accordingly, we compared the pheromone response in wild type cells and mutants defective in Gpa1 trafficking using MAPK activation and transcription reporter assays. In the case of Gpa1$^{\Delta UD}$, we replaced the wild type gene with the UD mutant via PCR-mediated integration. This was done at the endogenous *GPA1* locus so as to maintain proper G protein expression and subunit stoichiometry. As shown in Fig. 7*A*, there was no significant change in MAPK activation in the UBD mutants (*bul1*Δ, *ede1*Δ, *ddi1*Δ, and *rup1*Δ) when compared with wild type cells. Furthermore, we observed no significant differences when comparing the Gpa1$^{\Delta UD}$ mutant and wild type protein. Similarly, we observed only modest differences in the pheromone transcription response (Fig. 7*B*). Taken together, these data indicate that the MAPK branch of the pheromone pathway is largely unaffected by the trafficking-deficient mutants.

In addition to the MAPK and transcription response, the pheromone pathway has a second branch that activates the small G protein Cdc42. Active Cdc42 promotes polarization and morphogenesis to facilitate mating (59). We, therefore, asked whether defects in Gpa1 trafficking had any effect on cellular morphogenesis (shmoo formation). We monitored each mutant in a microfluidic chamber with constant pheromone stimulation, as previously described (42). At a saturating concentration of pheromone, wild type cells can form up to three mating projections. As shown in Fig. 7*C* there were no differences between wild type and *bul1*Δ, *ddi1*Δ, or *rup1*Δ mutants. Cells lacking Ede1 did exhibit an increased number of projections, as compared with wild type, but this same phenotype was evident in an *ede1*Δ Gpa1$^{\Delta UD}$ double mutant, indicating that the *ede1* phenotype is not the result of impaired Gpa1 trafficking. In contrast to all of the other strains tested, cells that express Gpa1$^{\Delta UD}$ were able to form just a single mating projection (Fig. 7*C*). These cells formed a shmoo and are subsequently elongated. Taken together these results suggest that Gpa1 must be endocytosed for proper morphogenesis to occur. Because the same morphological defect was not observed in the UBD deletion mutants, it is the first step of removing Gpa1 from the plasma membrane that is necessary for the formation of additional mating projections.

Finally, previous reports indicated that multiple projections are necessary for optimal mating efficiency (60). Accordingly, we observed a 2-fold higher mating efficiency in wild type as compared with the Gpa1$^{\Delta UD}$ mutant strain (Fig. 7*D*). Thus the cellular morphogenesis defects exhibited by ubiquitin-deficient Gpa1$^{\Delta UD}$ mutants leads to reduced mating fitness. Because we have shown that removal of the UD does not alter Gpa1 enzymatic activity or MAPK signaling, we conclude that monoubiquitination and removal from the plasma membrane contributes to proper morphogenesis and mating.

DISCUSSION

Here we have used biochemical, biophysical, genetic, and cell biological approaches to demonstrate a positive signaling role for Gα endocytosis. Taking advantage of the yeast system, we identified seven ubiquitin binding domain-containing proteins required for constitutive internalization of the G protein. Three of these proteins act on Ste2 as well as Gpa1. Four others act on Gpa1 alone, demonstrating that endocytosis of the G protein and receptor are distinct processes regulated by distinct binding partners. We further show that the Gpa1 UD is targeted by the UBD proteins. In the absence of the ubiquitination domain, Gpa1 is retained at the plasma membrane, and cellular morphogenesis is curtailed. A second effector pathway leading to MAPK activation is unaffected.

The proteins specifically required for Gpa1 trafficking (Rup1, Ddi1, Bul1, and Ede1) act at different stages of endocytosis (Fig. 8). Rup1 binds to Rsp5 and stimulates Rsp5 autocatalysis and substrate ubiquitination (58). We suggest that Rup1 may promote Rsp5-mediated ubiquitination of particular membrane proteins. Bul1 is the ubiquitin binding component of the Rsp5 ubiquitin ligase (55). Curiously, we find that Bul1, but not the closely related protein Bul2, promotes Gpa1 endocytosis. Even though Bul1 and Bul2 are homologous, they appear to have distinct functions within the cell. For example, Bul1 is a negative regulator of the tryptophan permease Tat2, but Bul2 is not (61, 62). Ddi1 is a DNA damage-inducible v-SNARE-binding protein (57) that was previously shown to be a negative regulator of the late secretory pathway, a function that is independent of the UBA domain of Ddi1 (63). Finally, Ede1 is a member of the epsin family of adapter proteins and a component of the early endocytic machinery (56, 61, 64, 65). Deletion of Ede1 but not other epsin proteins (Ent1, Ent2) leads to Gpa1 mislocaliza-

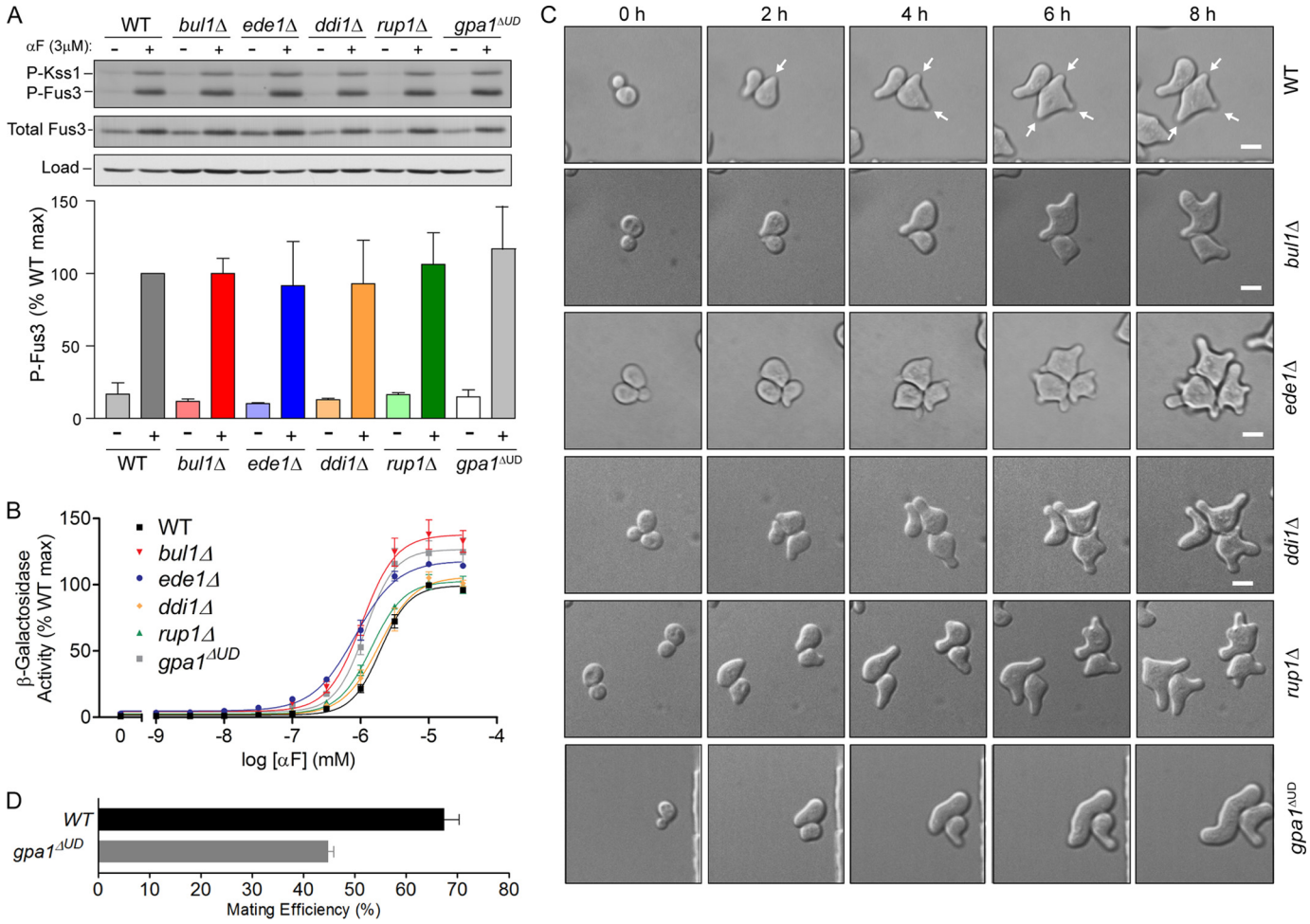

FIGURE 7. **Proper endocytosis of Gpa1 is required for sustained morphogenesis and efficient mating.** *A*, MAPK activation profiles. Wild type (WT) cells, *bul1*Δ, *ede1*Δ, *ddi1*Δ, *rup1*Δ, and *gpa1*$^{\Delta UD}$ were either left untreated or treated with 3 μM α-factor (α*F*) for 30 min. MAPK activation was determined by immunoblotting with phospho-MAPK p44/42 (*P-Fus3*, *P-Kss1*), Fus3 (*Total Fus3*) and G6PDH (*Load* control) antibodies. The image is representative of three independent experiments. *Bottom*, densitometry of P-Fus3 bands normalized to total Fus3. Results show the mean ± S.E. for three individual experiments. *B*, transcriptional activation (β-galactosidase activity) in response to α-factor treatment was measured spectrofluorometrically in wild type, *bul1*Δ, *ede1*Δ, *ddi1*Δ, *rup1*Δ, and *gpa1*$^{\Delta UD}$ cells. Strains were transformed with a *FUS1-lacZ* reporter and treated with the indicated concentrations of α-factor for 90 min. Data for the individual mutants were normalized to WT in each case. Results show the mean ± S.E. for three independent experiments, each performed in quadruplicate. *C*, loss of ubiquitination domain of Gpa1 results in morphological abnormalities under prolonged pheromone stimulation. Wild type *bul1*Δ, *ede1*Δ, *ddi1*Δ, *rup1*Δ, and *gpa1*$^{\Delta UD}$ cells were stimulated with a constant saturating dose (150 nM) of α-factor in a microfluidic chamber. Differential interference contrast images were taken every 5 min for 8 h to monitor changes in morphology. *Arrows* point to mating projections in wild type cells. *Scale bar*, 5 μm. *D*, mating efficiency assay. Separate cultures of wild type mating-type α cells (BY4742) and wild type or *gpa1*$^{\Delta UD}$ mating-type **a** cells (BY4741) were used. Cells from each culture were mixed and incubated for 4 h. Results are the mean ± S.E. from four replicates.

tion. Although Ede1 is implicated in Ste2 trafficking, we did not observe Ste2 mislocalization in the absence of Ede1. Ste2 trafficking has previously been monitored in agonist-stimulated cells. In contrast, we measured Gpa1 and Ste2 trafficking in unstimulated cells. Thus it is possible that Ede1 is important for pheromone-dependent, but not basal, trafficking of Ste2.

It is of note that when endocytosis of Gpa1 is inhibited (*rup1*Δ, *ddi1*Δ, *ede1*Δ), we could detect more of the monoubiquitinated protein and, in some cases, more polyubiquitinated Gpa1 as well. Differences in the levels of Gpa1 monoubiquitination and polyubiquitination likely reflect the roles of the UBD-containing proteins in the removal of monoubiquitinated substrates. When normal trafficking is abrogated, the monoubiquitinated species accumulates and may undergo additional ubiquitination steps resulting in the accumulation of polyubiquitinated substrate. Conversely, we observed no increase in the amount of ubiquitinated Gpa1 in the strain lacking *BUL1* despite the trafficking defect in that mutant. Because Bul1 is a ubiquitin binding component of the ubiquitin ligase Rsp5, it is possible that the ligase is unable to act effectively on Gpa1 when Bul1 is absent. Taken together these data suggest that the quantity of Gpa1 at the plasma membrane is finely tuned and that if Gpa1 cannot be removed through monoubiquitination and delivery to the vacuole, it is instead removed through polyubiquitination and delivery to the proteasome.

Our second major finding is that the UD promotes Gpa1 trafficking without altering Gpa1 enzymatic activity *in vitro* or MAPK activation *in vivo*. These results are particularly striking given that (*a*) the ubiquitination domain is located near a key dynamic region of the α-helical domain, (*b*) the ubiquitination domain is essential for transport of Gpa1 to the vacuole, and (*c*) there are a number of Gpa1 binding partners that specifically target the ubiquitination domain. These binding partners include enzymes responsible for monoubiquitination (Rsp5)

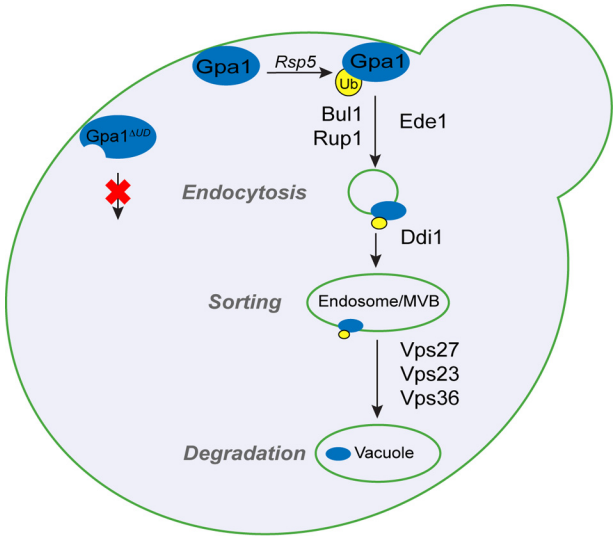

FIGURE 8. **Components required for proper endocytosis of Gpa1 after Rsp5-mediated monoubiquitination.** The predicted order of action of UBD-containing proteins involved in the trafficking of monoubiquitinated (Ub) Gpa1. When Gpa1 cannot be ubiquitinated ($Gpa1^{\Delta UD}$), it remains at the plasma membrane. Prolonged pheromone stimulation promotes formation of multiple mating projections in wild type but not mutant cells.

(26), polyubiquitination (SCF/Cdc4) (29), deubiquitination (Ubp12) (25), phosphorylation (Elm1, Tos1, Sak3) (30, 31, 66), and dephosphorylation (Reg1) (66) as well as the seven UBD proteins identified here. We conclude that the ubiquitination domain likely evolved to serve a unique trafficking function and that this function is wholly separate from the regulation of G protein catalytic activity.

Although the UD is unique to yeast Gα proteins, Gα trafficking is not. Trafficking of Gα has long been established in the visual system, where a redistribution of the protein serves to decrease signaling, allowing adaptation to bright light (67). Whereas the visual Gα acts directly to stimulate an effector enzyme, yeast Gpa1 acts indirectly to sequester Gβγ and prevent downstream signaling. Therefore, the final outcome of Gα endocytosis will be different in the visual and yeast signaling systems. Gα endocytosis attenuates signaling in the visual system but promotes signaling in the yeast mating pathway. On the other hand, Gα proteins have been shown to be activated at the endosomal membrane compartment both in yeast and in mammalian cells (12, 14). Before our analysis, however, little was known about the proteins necessary for proper Gα trafficking.

Finally, our analysis of the UD may lead to insights regarding the function of unique inserts in other signaling proteins. For example, there are families of small GTPases that are known to contain inserts within the highly conserved Ras-like domains. Members of the Rho family of small GTPases have a unique insert, called the Rho insert, that is not present in other small GTPases (68). The presence or absence of the Rho insert does not alter the intrinsic activity of these small GTPases (69). However, when the insert is absent Rho can bind, but no longer activate, its downstream effector Rho kinase (69). The Rho insert in the small GTPase Rac1 was recently shown to be monoubiquitinated (70). Although no function has yet been assigned to monoubiquitination of Rac1, it is possible that this modification is involved in the mechanism by which Rho interacts with downstream effectors. Monoubiquitination of mammalian Ras proteins can lead to cell transformation (71) and does so by promoting nucleotide exchange or by impeding the binding of the GTPase activating protein (72, 73).

In summary we have identified four UBD-containing proteins as specific regulators of G protein trafficking. When trafficking is abrogated, the morphogenesis branch of the pathway is attenuated. None of these UBD proteins affect the MAPK branch of the signaling pathway, and none affect trafficking of the receptor. Looking forward, our integrated approach should be broadly applicable as more ubiquitination substrates, ubiquitination domains, and UBD-containing proteins are identified. Recently, dysregulation of NEDD4/Rsp5-mediated trafficking was shown to promote neurodegenerative disease (20). In view of these findings, any components responsible for monoubiquitination and protein trafficking represent potential targets for future drug development efforts.

Acknowledgments—We thank Brenda Temple for providing the G protein sequence alignment, Daniel Isom for help with cysteine labeling, David Smalley for help with mass spectrometry, Sarah Clement for the $Gpa1^{\Delta UD}$ strain construction, and Ash Tripathy for help with circular dichroism. We also thank Yuqi Wang and Patrick Brennwald for critical reading of the manuscript.

REFERENCES

1. Sprang, S. R. (1997) G protein mechanisms: insights from structural analysis. *Annu. Rev. Biochem.* **66,** 639–678
2. Ross, E. M., and Wilkie, T. M. (2000) GTPase-activating proteins for heterotrimeric G proteins: regulators of G protein signaling (RGS) and RGS-like proteins. *Annu. Rev. Biochem.* **69,** 795–827
3. Berman, D. M., Wilkie, T. M., and Gilman, A. G. (1996) GAIP and RGS4 Are GTPase-activating proteins for the G_i subfamily of G protein ± subunits. *Cell* **86,** 445–452
4. Dohlman, H. G., and Jones, J. C. (2012) Signal activation and inactivation by the Gα helical domain: a long-neglected partner in G protein signaling. *Sci. Signal.* **5,** re2
5. Mixon, M. B., Lee, E., Coleman, D. E., Berghuis, A. M., Gilman, A. G., and Sprang, S. R. (1995) Tertiary and quaternary structural changes in $G_i\alpha$ induced by GTP hydrolysis. *Science* **270,** 954–960
6. Westfield, G. H., Rasmussen, S. G., Su, M., Dutta, S., DeVree, B. T., Chung, K. Y., Calinski, D., Velez-Ruiz, G., Oleskie, A. N., Pardon, E., Chae, P. S., Liu, T., Li, S., Woods, V. L., Jr., Steyaert, J., Kobilka, B. K., Sunahara, R. K., and Skiniotis, G. (2011) Structural flexibility of the $G\alpha_s$ α-helical domain in the β2-adrenoceptor G_s complex. *Proc. Natl. Acad. Sci. U.S.A.* **108,** 16086–16091
7. Van Eps, N., Preininger, A. M., Alexander, N., Kaya, A. I., Meier, S., Meiler, J., Hamm, H. E., and Hubbell, W. L. (2011) Interaction of a G protein with an activated receptor opens the interdomain interface in the α subunit. *Proc. Natl. Acad. Sci. U.S.A.* **108,** 9420–9424
8. Wedegaertner, P. B. (2012) G protein trafficking. In *GPCR Signalling Complexes-Synthesis, Assembly, Trafficking, and Specificity* (Dupré, D. J., Hébert, T. E., and Jockers, R., eds.) pp. 193–223, Springer, The Netherlands
9. Frechter, S., Elia, N., Tzarfaty, V., Selinger, Z., and Minke, B. (2007) Translocation of $G_q\alpha$ mediates long-term adaptation in *Drosophila* photoreceptors. *J. Neurosci.* **27,** 5571–5583
10. Chisari, M., Saini, D. K., Kalyanaraman, V., and Gautam, N. (2007) Shuttling of G protein subunits between the plasma membrane and intracellular membranes. *J. Biol. Chem.* **282,** 24092–24098
11. Wedegaertner, P. B., Bourne, H. R., and von Zastrow, M. (1996) Activation-induced subcellular redistribution of $G_s\alpha$. *Mol. Biol. Cell* **7,**

1225–1233
12. Slessareva, J. E., Routt, S. M., Temple, B., Bankaitis, V. A., and Dohlman, H. G. (2006) Activation of the phosphatidylinositol 3-kinase Vps34 by a G protein α subunit at the endosome. *Cell* **126,** 191–203
13. Backer, J. M. (2008) The regulation and function of Class III PI3Ks: novel roles for Vps34. *Biochem. J.* **410,** 1–17
14. Irannejad, R., Tomshine, J. C., Tomshine, J. R., Chevalier, M., Mahoney, J. P., Steyaert, J., Rasmussen, S. G., Sunahara, R. K., El-Samad, H., Huang, B., and von Zastrow, M. (2013) Conformational biosensors reveal GPCR signalling from endosomes. *Nature* **495,** 534–538
15. Murphy, J. E., Padilla, B. E., Hasdemir, B., Cottrell, G. S., and Bunnett, N. W. (2009) Endosomes: a legitimate platform for the signaling train. *Proc. Natl. Acad. Sci. U.S.A.* **106,** 17615–17622
16. Hicke, L., and Riezman, H. (1996) Ubiquitination of a yeast plasma membrane receptor signals its ligand-stimulated endocytosis. *Cell* **84,** 277–287
17. Hicke, L. (1999) Gettin' down with ubiquitin: turning off cell-surface receptors, transporters, and channels. *Trends Cell Biol.* **9,** 107–112
18. Zhu, M., Torres, M. P., Kelley, J. B., Dohlman, H. G., and Wang, Y. (2011) Pheromone- and RSP5-dependent ubiquitination of the G protein β subunit Ste4 in yeast. *J. Biol. Chem.* **286,** 27147–27155
19. Shaw, J. D., Cummings, K. B., Huyer, G., Michaelis, S., and Wendland, B. (2001) Yeast as a model system for studying endocytosis. *Exp. Cell Res.* **271,** 1–9
20. Tardiff, D. F., Jui, N. T., Khurana, V., Tambe, M. A., Thompson, M. L., Chung, C. Y., Kamadurai, H. B., Kim, H. T., Lancaster, A. K., Caldwell, K. A., Caldwell, G. A., Rochet, J.-C., Buchwald, S. L., and Lindquist, S. (2013) Yeast reveal a "Druggable" Rsp5/Nedd4 network that ameliorates α-synuclein toxicity in neurons. *Science* **342,** 979–983
21. Shih, S. C., Sloper-Mould, K. E., and Hicke, L. (2000) Monoubiquitin carries a novel internalization signal that is appended to activated receptors. *EMBO J.* **19,** 187–198
22. Sloper-Mould, K. E., Jemc, J. C., Pickart, C. M., and Hicke, L. (2001) Distinct functional surface regions on ubiquitin. *J. Biol. Chem.* **276,** 30483–30489
23. Husnjak, K., and Dikic, I. (2012) Ubiquitin-binding proteins: decoders of ubiquitin-mediated cellular functions. *Annu. Rev. Biochem.* **81,** 291–322
24. Dohlman, H. G., and Thorner, J. (2001) Regulation of G protein initiated signal transduction in yeast: paradigms and principles. *Annu. Rev. Biochem.* **70,** 703–754
25. Wang, Y., Marotti, L. A., Jr., Lee, M. J., and Dohlman, H. G. (2005) Differential regulation of G protein α subunit trafficking by mono- and polyubiquitination, *J. Biol. Chem.* **280,** 284–291
26. Torres, M. P., Lee, M. J., Ding, F., Purbeck, C., Kuhlman, B., Dokholyan, N. V., and Dohlman, H. G. (2009) G protein mono-ubiquitination by the Rsp5 ubiquitin ligase. *J. Biol. Chem.* **284,** 8940–8950
27. Dunn, R., and Hicke, L. (2001) Domains of the Rsp5 ubiquitin-protein ligase required for receptor-mediated and fluid-phase endocytosis. *Mol. Biol. Cell* **12,** 421–435
28. Marotti, L. A., Jr., Newitt, R., Wang, Y., Aebersold, R., and Dohlman, H. G. (2002) Direct identification of a G protein ubiquitination site by mass spectrometry. *Biochemistry* **41,** 5067–5074
29. Cappell, S. D., Baker, R., Skowyra, D., and Dohlman, H. G. (2010) Systematic analysis of essential genes reveals important regulators of G protein signaling. *Mol. Cell* **38,** 746–757
30. Li, X., Gerber, S. A., Rudner, A. D., Beausoleil, S. A., Haas, W., Villén, J., Elias, J. E., and Gygi, S. P. (2007) Large-scale phosphorylation analysis of α-factor-arrested *Saccharomyces cerevisiae*. *J. Proteome Res.* **6,** 1190–1197
31. Torres, M. P., Clement, S. T., Cappell, S. D., and Dohlman, H. G. (2011) Cell cycle-dependent phosphorylation and ubiquitination of a G protein α subunit. *J. Biol. Chem.* **286,** 20208–20216
32. Coleman, D. E., Berghuis, A. M., Lee, E., Linder, M. E., Gilman, A. G., and Sprang, S. R. (1994) Structures of active conformations of $G_i\alpha_1$ and the mechanism of GTP hydrolysis. *Science* **265,** 1405–1412
33. Hoffman, G. A., Garrison, T. R., and Dohlman, H. G. (2002) Analysis of RGS proteins in *Saccharomyces cerevisiae*. *Methods Enzymol.* **344,** 617–631
34. Song, J., Hirschman, J., Gunn, K., and Dohlman, H. G. (1996) Regulation of membrane and subunit interactions by N-myristoylation of a G protein α subunit in yeast. *J. Biol. Chem.* **271,** 20273–20283
35. Clarke, T. F., 4th, and Clark, P. L. (2008) Rare codons cluster. *PLoS ONE* **3,** e3412
36. Isom, D. G., Sridharan, V., Baker, R., Clement, S. T., Smalley, D. M., and Dohlman, H. G. (2013) Protons as second messenger regulators of G protein signaling. *Mol. Cell* **51,** 531–538
37. Isom, D. G., Marguet, P. R., Oas, T. G., and Hellinga, H. W. (2011) A miniaturized technique for assessing protein thermodynamics and function using fast determination of quantitative cysteine reactivity. *Proteins* **79,** 1034–1047
38. Brachmann, C. B., Davies, A., Cost, G. J., Caputo, E., Li, J., Hieter, P., and Boeke, J. D. (1998) Designer deletion strains derived from *Saccharomyces cerevisiae* S288C: a useful set of strains and plasmids for PCR-mediated gene disruption and other applications. *Yeast* **14,** 115–132
39. Wach, A., Brachat, A., Pöhlmann, R., and Philippsen, P. (1994) New heterologous modules for classical or PCR-based gene disruptions in *Saccharomyces cerevisiae*. *Yeast* **10,** 1793–1808
40. Lee, M. J., and Dohlman, H. G. (2008) Coactivation of G protein signaling by cell-surface receptors and an intracellular exchange factor. *Curr. Biol.* **18,** 211–215
41. Dohlman, H. G., Goldsmith, P., Spiegel, A. M., and Thorner, J. (1993) Pheromone action regulates G-protein α-subunit myristoylation in the yeast *Saccharomyces cerevisiae*. *Proc. Natl. Acad. Sci. U.S.A.* **90,** 9688–9692
42. Hao, N., Nayak, S., Behar, M., Shanks, R. H., Nagiec, M. J., Errede, B., Hasty, J., Elston, T. C., and Dohlman, H. G. (2008) Regulation of cell signaling dynamics by the protein kinase-scaffold Ste5. *Mol. Cell* **30,** 649–656
43. Sprague, G. F., Jr. (1991) Assay of yeast mating reaction. *Methods Enzymol.* **194,** 77–93
44. Radivojac, P., Vacic, V., Haynes, C., Cocklin, R. R., Mohan, A., Heyen, J. W., Goebl, M. G., and Iakoucheva, L. M. (2010) Identification, analysis, and prediction of protein ubiquitination sites. *Proteins* **78,** 365–380
45. Jones, J. C., Jones, A. M., Temple, B. R., and Dohlman, H. G. (2012) Differences in intradomain and interdomain motion confer distinct activation properties to structurally similar Gα proteins. *Proc. Natl. Acad. Sci. U.S.A.* **109,** 7275–7279
46. Higashijima, T., Ferguson, K. M., Sternweis, P. C., Ross, E. M., Smigel, M. D., and Gilman, A. G. (1987) The effect of activating ligands on the intrinsic fluorescence of guanine nucleotide-binding regulatory proteins. *J. Biol. Chem.* **262,** 752–756
47. Hurley, J. H., and Stenmark, H. (2011) Molecular mechanisms of ubiquitin-dependent membrane traffic. *Annu. Rev. Biophys.* **40,** 119–142
48. Hicke, L., Schubert, H. L., and Hill, C. P. (2005) Ubiquitin-binding domains. *Nat. Rev. Mol. Cell. Biol.* **6,** 610–621
49. Dikic, I., Wakatsuki, S., and Walters, K. J. (2009) Ubiquitin-binding domains: from structures to functions. *Nat. Rev. Mol. Cell Biol.* **10,** 659–671
50. Winzeler, E. A., Shoemaker, D. D., Astromoff, A., Liang, H., Anderson, K., Andre, B., Bangham, R., Benito, R., Boeke, J. D., Bussey, H., Chu, A. M., Connelly, C., Davis, K., Dietrich, F., Dow, S. W., El Bakkoury, M., Foury, F., Friend, S. H., Gentalen, E., Giaever, G., Hegemann, J. H., Jones, T., Laub, M., Liao, H., Liebundguth, N., Lockhart, D. J., Lucau-Danila, A., Lussier, M., M'Rabet, N., Menard, P., Mittmann, M., Pai, C., Rebischung, C., Revuelta, J. L., Riles, L., Roberts, C. J., Ross-MacDonald, P., Scherens, B., Snyder, M., Sookhai-Mahadeo, S., Storms, R. K., Véronneau, S., Voet, M., Volckaert, G., Ward, T. R., Wysocki, R., Yen, G. S., Yu, K., Zimmermann, K., Philippsen, P., Johnston, M., and Davis, R. W. (1999) Functional characterization of the *S. cerevisiae* genome by gene deletion and parallel analysis. *Science* **285,** 901–906
51. Hurley, J. H. (2010) The ESCRT complexes. *Crit. Rev. Biochem. Mol. Biol.* **45,** 463–487
52. MacGurn, J. A., Hsu, P.-C., and Emr, S. D. (2012) Ubiquitin and membrane protein turnover: from cradle to grave. *Annu. Rev. Biochem.* **81,** 231–259
53. Donaldson, K. M., Yin, H., Gekakis, N., Supek, F., and Joazeiro, C. A. (2003) Ubiquitin signals protein trafficking via interaction with a novel ubiquitin binding domain in the membrane fusion regulator, Vps9p. *Curr. Biol.* **13,** 258–262

54. Betz, W. J., Mao, F., and Smith, C. B. (1996) Imaging exocytosis and endocytosis. *Curr. Opin. Neurobiol.* **6,** 365–371
55. Yashiroda, H., Oguchi, T., Yasuda, Y., Toh-E. A., and Kikuchi, Y. (1996) Bul1, a new protein that binds to the Rsp5 ubiquitin ligase in *Saccharomyces cerevisiae*. *Mol. Cell. Biol.* **16,** 3255–3263
56. Gagny, B., Wiederkehr, A., Dumoulin, P., Winsor, B., Riezman, H., and Haguenauer-Tsapis, R. (2000) A novel EH domain protein of *Saccharomyces cerevisiae*, Ede1p, involved in endocytosis. *J. Cell Sci.* **113,** 3309–3319
57. Liu, Y., and Xiao, W. (1997) Bidirectional regulation of two DNA-damage-inducible genes, MAG1 and DDI1, from *Saccharomyces cerevisiae*. *Mol. Microbiol.* **23,** 777–789
58. Lam, M. H., and Emili, A. (2013) Ubp2 regulates Rsp5 ubiquitination activity *in vivo* and *in vitro*. *PLoS ONE* **8,** e75372
59. Pruyne, D., and Bretscher, A. (2000) Polarization of cell growth in yeast. *J. Cell Sci.* **113,** 571–585
60. Tanaka, H., and Yi, T.-M. (2010) The effects of replacing Sst2 with the heterologous RGS4 on polarization and mating in yeast. *Biophys. J.* **99,** 1007–1017
61. Abe, F., and Iida, H. (2003) Pressure-induced differential regulation of the two tryptophan permeases Tat1 and Tat2 by ubiquitin ligase Rsp5 and its binding proteins, Bul1 and Bul2. *Mol. Cell. Biol.* **23,** 7566–7584
62. Hiraki, T., and Abe, F. (2010) Overexpression of Sna3 stabilizes tryptophan permease Tat2, potentially competing for the WW domain of Rsp5 ubiquitin ligase with its binding protein Bul1. *FEBS Lett.* **584,** 55–60
63. Gabriely, G., Kama, R., Gelin-Licht, R., and Gerst, J. E. (2008) Different domains of the UBL-UBA ubiquitin receptor, Ddi1/Vsm1, are involved in its multiple cellular roles. *Mol. Biol. Cell* **19,** 3625–3637
64. Dores, M. R., Schnell, J. D., Maldonado-Baez, L., Wendland, B., and Hicke, L. (2010) The function of yeast epsin and Ede1 ubiquitin-binding domains during receptor internalization. *Traffic* **11,** 151–160
65. Shih, S. C., Katzmann, D. J., Schnell, J. D., Sutanto, M., Emr, S. D., and Hicke, L. (2002) Epsins and Vps27p/Hrs contain ubiquitin-binding domains that function in receptor endocytosis. *Nat. Cell Biol.* **4,** 389–393
66. Clement, S. T., Dixit, G., and Dohlman, H. G. (2013) Regulation of yeast G protein signaling by the kinases that activate the AMPK homolog Snf1. *Sci. Signal.* **6,** ra78
67. Sokolov, M., Lyubarsky, A. L., Strissel, K. J., Savchenko, A. B., Govardovskii, V. I., Pugh, E. N., Jr., and Arshavsky, V. Y. (2002) Massive light-driven translocation of transducin between the two major compartments of rod cells: a novel mechanism of light adaptation. *Neuron* **34,** 95–106
68. Rojas, A. M., Fuentes, G., Rausell, A., and Valencia, A. (2012) The Ras protein superfamily: evolutionary tree and role of conserved amino acids. *J. Cell Biol.* **196,** 545
69. Zong, H., Kaibuchi, K., and Quilliam, L. A. (2001) The insert region of RhoA is essential for Rho kinase activation and cellular transformation. *Mol. Cell. Biol.* **21,** 5287–5298
70. Visvikis, O., Lorès, P., Boyer, L., Chardin, P., Lemichez, E., and Gacon, G. (2008) Activated Rac1, but not the tumorigenic variant Rac1b, is ubiquitinated on Lys-147 through a JNK-regulated process. *FEBS J.* **275,** 386–396
71. Sasaki, A. T., Carracedo, A., Locasale, J. W., Anastasiou, D., Takeuchi, K., Kahoud, E. R., Haviv, S., Asara, J. M., Pandolfi, P. P., and Cantley, L. C. (2011) Ubiquitination of K-Ras enhances activation and facilitates binding to select downstream effectors. *Sci. Signal.* **4,** ra13
72. Baker, R., Wilkerson, E. M., Sumita, K., Isom, D. G., Sasaki, A. T., Dohlman, H. G., and Campbell, S. L. (2013) Differences in the regulation of K-Ras and H-Ras isoforms by monoubiquitination. *J. Biol. Chem.* **288,** 36856–36862
73. Baker, R., Lewis, S. M., Sasaki, A. T., Wilkerson, E. M., Locasale, J. W., Cantley, L. C., Kuhlman, B., Dohlman, H. G., and Campbell, S. L. (2013) Site-specific monoubiquitination activates Ras by impeding GTPase-activating protein function. *Nat. Struct. Mol. Biol.* **20,** 46–52